PHYSICAL REVIEW B VOLUME 52, NUMBER 6 1 AUGUST 1995-II

Phonons in $CuGeO_3$ studied using polarized far-infrared and Raman-scattering spectroscopies

Z. V. Popović and S. D. Dević
Institute of Physics, 11 001 Belgrade, P.O. Box 57, Yugoslavia

V. N. Popov
Faculty of Physics, University of Sofia, 1126 Sofia, Bulgaria

G. Dhalenne and A. Revcolevschi
Laboratoire De Chimie Solides, Université de Paris Sud, Bâtiment 414, 91405 Orsay, France
(Received 17 February 1995)

Optical phonons in $CuGeO_3$ were studied using polarized far-infrared and Raman-scattering spectroscopies. The frequencies of the infrared-active modes are determined using an oscillator-fitting procedure of reflectivity data. All infrared and Raman active modes, predicted by factor-group analysis, were observed. The assignment of the observed phonons is given according to Cartesian symmetry coordinates as well as preliminary lattice dynamical calculations on the basis of a shell model.

I. INTRODUCTION

The recent discovery[1] of the spin-Peierls phase transition in inorganic compound $CuGeO_3$ has led to rapidly increasing interest for investigation of the various physical properties of this material.[2–5] The copper metagermanate ($CuGeO_3$) has an orthorhombic crystal structure with lattice parameters $a=0.481$ nm, $b=0.847$ nm, and $c=0.294$ nm, $Z=2$ and the space group *Pbmm*.[6] A schematic representation of the crystal structure of this oxide is given in Fig. 1. The basic building blocks of the $CuGeO_3$ structure are corner-sharing GeO_4 tetrahedra that forms $(GeO_3^{2-})_n$ chains. These chains are linked by Cu^{2+} ions. Each Cu atom is surrounded by six oxygen atoms, forming strongly deformed CuO_6 octahedron. Two $(GeO_3^{2-})_n$ chains comprising the $CuGeO_3$ unit cell are along the c axis of the crystal.

Phonon properties of this compound are poorly studied. The unpolarized Raman and infrared transmission spectra were measured on polycrystalline samples[7] at room and liquid-nitrogen temperatures. The Raman-scattering spectra of $CuGeO_3$ in spin-Peierls phase are discussed in Refs. 8 and 9. In our earlier paper[10] the polarized Raman and infrared-reflectivity spectra are given in the temperature range between 10 and 300 K. The assignment of the observed 12 Raman and 7 infrared-active modes was given on the basis of the factor-group and normal coordinate analyses.

In this work we present far-infrared reflectivity as well as Raman-scattering spectra for all principal polarizations. All optical modes predicted by factor-group analysis are experimentally observed. The assignment of the vibrational modes is given according to Cartesian symmetry coordinates as well as preliminary force-constant calculations on the basis of a shell model.

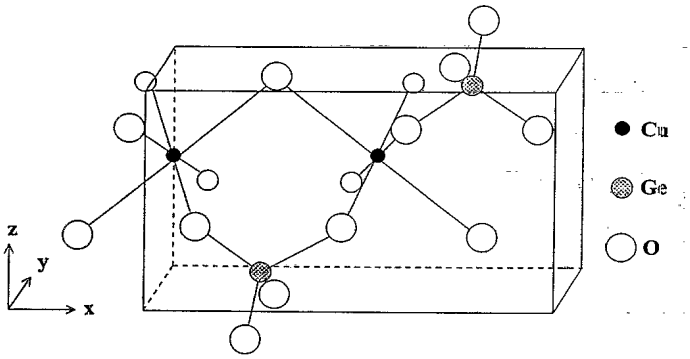

FIG. 1. Schematic representation of the $CuGeO_3$ crystal structure. The axes orientation is changed from *Pbmm* setting (Ref. 6) ($x=b$; $y=c$; $z=a$) into a standard setting ($x=a$; $y=b$; $z=c$).

II. EXPERIMENT

The $CuGeO_3$ single crystal used in this study was cleaved from cylindrical crystals, 6 mm in diameter and 8 cm long, grown from the melt by a floating zone method.[11] The sample used for spectroscopic measurements was $4\times5\times3$ mm^3 in size. The orientation of the principal axes was obtained by conventional Laue photographs.

The polarized far-infrared reflection (FIR) measurements were made in the spectral range from 30 to 1000 cm^{-1} at room temperature using both a Bruker IFS-113v spectrometer (in the spectral range 30–650 cm^{-1}) and Bruker IFS 66 spectrometer (for spectral range 400–4000 cm^{-1}).

The Raman spectra were excited by the 514.5-nm line of an argon-ion laser (the average power was about 100 mW), focused to a line using cylindrical lens. The geometry was a quasi-back-scattering with an aperture f of the collecting objective of 1:1.4. The monochromator used was a Jobin-Yvon model U 1000 with 1800 groves per mm holographic gratings. As a detector we used a Pelletier-effect-cooled RCA 31034 A photomultiplier with a conventional photon-counting system.

0163-1829/95/52(6)/4185(6)/$06.00

III. RESULTS AND DISCUSSION

A. Factor-group analysis (FGA)

As previously mentioned, the $CuGeO_3$ unit cell consists of two formula units comprising 10 atoms in all. The parameters of the unit cell, originally taken from Ref. 6, were adapted to the standard setting for *Pmma* space group. Parameters of the unit cell in this case are $a'=b=x$, $b'=c=y$, $c'=a=z$ (see Fig. 1). Further analysis of the vibrational properties will be proceeded according to this standard setting.

The factor group analysis, using tables given by Rousseau,[12] yields

$$\mathrm{Cu}(C_{2h}):\ \Gamma = A_u + 2B_{1u} + B_{2u} + 3B_{3u}\ ,$$

$$\mathrm{Ge}(C_{2v}):\ \Gamma = A_g + B_{1u} + B_{2g} + B_{2u} + B_{3g} + B_{3u}\ ,$$

$$\mathrm{O}_1(C_{2v}):\ \Gamma = A_g + B_{1u} + B_{2g} + B_{2u} + B_{3g} + B_{3u}\ ,$$

$$\mathrm{O}_2(C_s):\ \Gamma = 2A_g + A_u + B_{1g} + 2B_{1u} + 2B_{2g} + B_{2u} + B_{3g} + 2B_{3u}\ .$$

Summarizing the representations given above and substracting acoustic $(B_{1u}+B_{2u}+B_{3u})$ and silent $(2A_u)$ modes, we obtain the irreducible representations of $CuGeO_3$ vibrational modes:[10]

$$\Gamma^{\mathrm{vib}}_{\mathrm{CuGeO_3}} = 4A_g(xx,yy,zz) + B_{1g}(xy) + 4B_{2g}(xz) + 3B_{3g}(yz) + 5B_{1u}(\mathbf{E}\|z) + 3B_{2u}(\mathbf{E}\|y) + 5B_{3u}(\mathbf{E}\|x)\ .$$

Thus, 12 Raman $(A_g, B_{1g}, B_{2g}, B_{3g})$ and 13 infrared (B_{1u}, B_{2u}, B_{3u}) active modes are to be expected in the $CuGeO_3$ spectra.

B. Infrared and Raman spectra

The polarized room-temperature far-infrared reflectivity spectra of $CuGeO_3$, in the spectral range from 30 to 1000 cm^{-1}, are given in Fig. 2. The open circles are experimental data and the solid lines represent the spectra computed using the four-parameter model for the dielectric constant:

$$\varepsilon = \varepsilon_\infty \prod_{j=1}^{n} \frac{\omega_{\mathrm{LO},j}^2 - \omega^2 + i\gamma_{\mathrm{LO},j}\omega}{\omega_{\mathrm{TO},j}^2 - \omega^2 + i\gamma_{\mathrm{TO},j}\omega}\ ,$$

where $\omega_{\mathrm{TO},j}$ and $\omega_{\mathrm{LO},j}$ are the transverse and longitudinal frequencies of the j^{th} oscillator, $\gamma_{\mathrm{TO},j}$ and $\gamma_{\mathrm{LO},j}$ are their corresponding dampings, and ε_∞ is the high-frequency dielectric constant. The best-oscillator-fit parameters are listed in Table I. The static dielectric constant, given in Table I, is obtained using the generalized Lyddane-Sachs-Teller (LST) relation $\varepsilon_0 = \varepsilon_\infty \prod_{j=1}^{n} \omega_{\mathrm{LO},j}^2 / \omega_{\mathrm{TO},j}^2$.

As can be seen from Fig. 2(a), the agreement between the observed and calculated reflectivity spectra for $\mathbf{E}\|z$ polarization is rather good. The disagreement between these spectra occurs only in the (400–600) cm^{-1} and (700–800) cm^{-1} ranges, due to leakage of the $\mathbf{E}\|y$ oscillators with $\omega_{\mathrm{TO}}=530$ and 720 cm^{-1}. This spectrum was obtained from the surface normal to the layers, whose quality is poorer than layer surface and some leakage of other polarization modes could be expected. For this polarization FGA predicts five modes and five modes are clearly observed. For $\mathbf{E}\|y$ polarization, Fig. 2(b), three modes of B_{2u} symmetry with TO frequencies at 165, 530, and 720 cm^{-1} are observed. In Fig. 2(c), the room-temperature reflectivity spectra of $CuGeO_3$ for $\mathbf{E}\|x$ polarization are shown. Four oscillators are clearly observed for this polarization in our earlier paper.[10] The fifth oscillator, located at about 48 cm^{-1}, was masked with interference fringes in measurements presented in Ref. 10.

Polarized room-temperature Raman spectra of $CuGeO_3$ in the spectral range between 30 and 1000 cm^{-1} are shown in Fig. 3. All Raman active modes, predicted by FGA are clearly seen. The frequencies of these modes with their symmetries are collected in Table I.

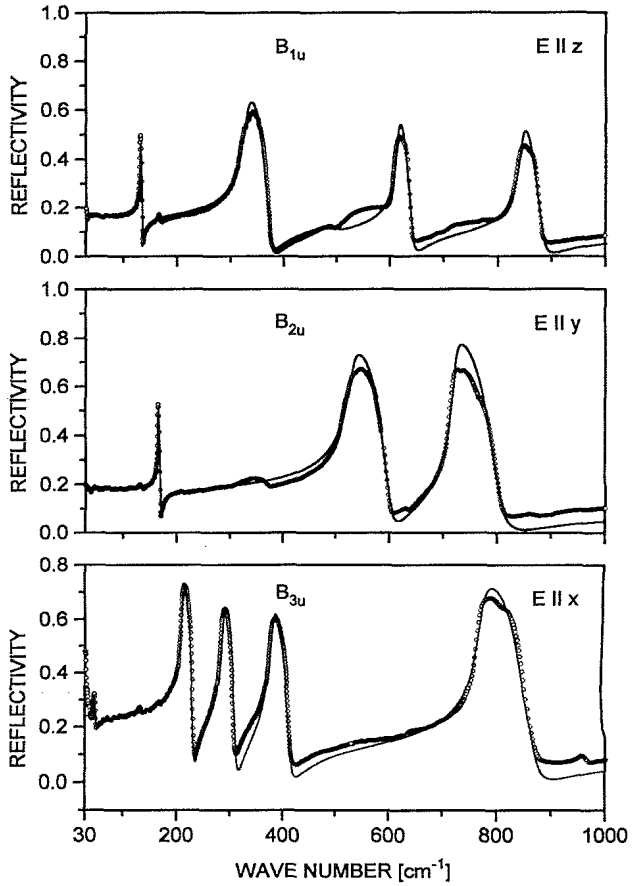

FIG. 2. Room-temperature far-infrared reflectivity spectra of $CuGeO_3$ single crystals in the spectral range 30–1000 cm^{-1} for (a) $E\|z$, (b) $E\|y$, and (c) $E\|x$ polarizations. The experimental values are given by open circles. The solid lines represent the calculated spectra obtained by a fitting procedure described in text.

TABLE I. Room-temperature frequencies of infrared and Raman active modes of $CuGeO_3$.

Mode	ω_{TO} (cm^{-1})	γ_{TO} (cm^{-1})	ω_{LO} (cm^{-1})	γ_{LO} (cm^{-1})	ε_0	ε_∞
B_{1u}	131	2	134	2		
	328	15	372	17		
	478	25	489	30	5.8	3.5
	615	10	640	17		
	843	15	880	25		
B_{2u}	165	1.5	168	2.5		
	530	15	600	30	5.0	3.0
	720	9	803	40		
B_{3u}	48	3	49	4		
	211	6	231	8		
	285	9	308	10	8.2	3.8
	377	12	414	17		
	772	15	857	25		

A_g	187	B_{1g}	388	B_{2g}	116	B_{3g}	110
	332				224		411
	594				427		712
	859				879		

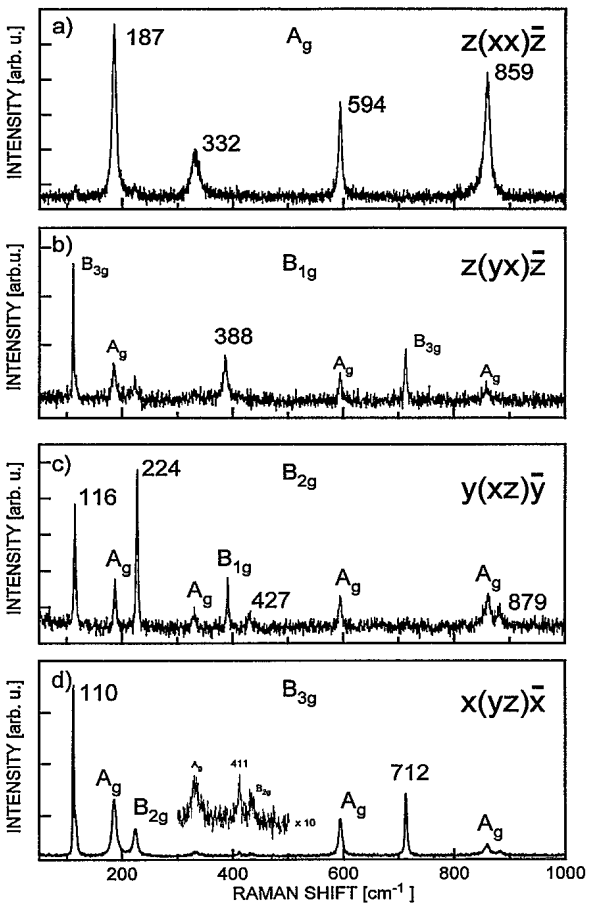

FIG. 3. Room-temperature Raman spectra of $CuGeO_3$ in (a) $z(xx)\bar{z}$, (b) $z(yx)\bar{z}$, (c) $y(xz)\bar{y}$ and $x(yz)\bar{x}$ polarizations.

C. Normal coordinate analysis

In order to assign the vibrational modes of $CuGeO_3$, the calculations of the lattice dynamics were carried out using a shell model. The initial values of model parameters for the ions Cu^{2+} and O^{2-}, as well as those for the ionic pairs Cu^{2+}-O^{2-} and O^{2-}-O^{2-} were taken from a previous study of monoclinic CuO.[13] These parameters were subsequently varied only slightly to reach agreement with some of the measured phonon frequencies. The remaining parameters for Ge^{4+} and the short-range Ge^{4+}-O^{2-} interactions were determined using the equilibrium conditions (vanishing of stresses and forces).

The short-range (SR) interactions were accounted for only between the ionic pairs given in Table II. The introduction of the Cu-O_1 SR interaction was essential for the stability of the model (as in the case with CuO), while the introduction of the Cu-O_2 (next-nearest-neighbor) SR interaction was needed in order to "raise" the frequency of the lowest B_{2g} mode from 60 cm^{-1}.

The calculated phonon frequencies together with the experimental ones and ionic displacement patterns are displayed in Fig. 4. Everywhere the disagreement between them is less than 10% and the deviation in the worst cases does not exceed 40 cm^{-1}.

TABLE II. Ionic pairs with nonzero SR interactions.

Ionic pair	Distance (Å)
Cu-O_1	2.766
Cu-O_2	1.942
Ge-O_1	1.769
Ge-O_2	1.724
Ge-O_2	3.304

As can be seen in Fig. 4(a), the A_g modes have (ac) polarization. The first mode at 187 cm^{-1} originates from in-phase vibration of Ge and O atoms of $(GeO_3^{2-})_n$ chains along the c axis. The second A_g mode at 332 cm^{-1} dominantly comes from (O_2) oxygen vibration which tends to rotate CuO_4 square. The A_g mode at 594 cm^{-1} originates from (O_1) oxygen bond-stretching vibration along the c axis and the last A_g mode at 859 cm^{-1} is the full-symmetric mode of oxygen vibration in CuO_4 square. As an illustration of polarization dependence of A_g modes in Fig. 5 we show the Raman spectra of $CuGeO_3$ for (xx) and (zz) polarization configurations. As can be seen from Fig. 5, in the case of (zz) polarization configuration the intensity of the A_g^1 mode is 10 times higher than the intensity of the A_g^2 mode. The same is valid for comparison of the intensity of the A_g^3 and A_g^4 modes. The A_g^3 and A_g^4 modes have near the same intensity in (xx) polarization, but in (zz) polariza-

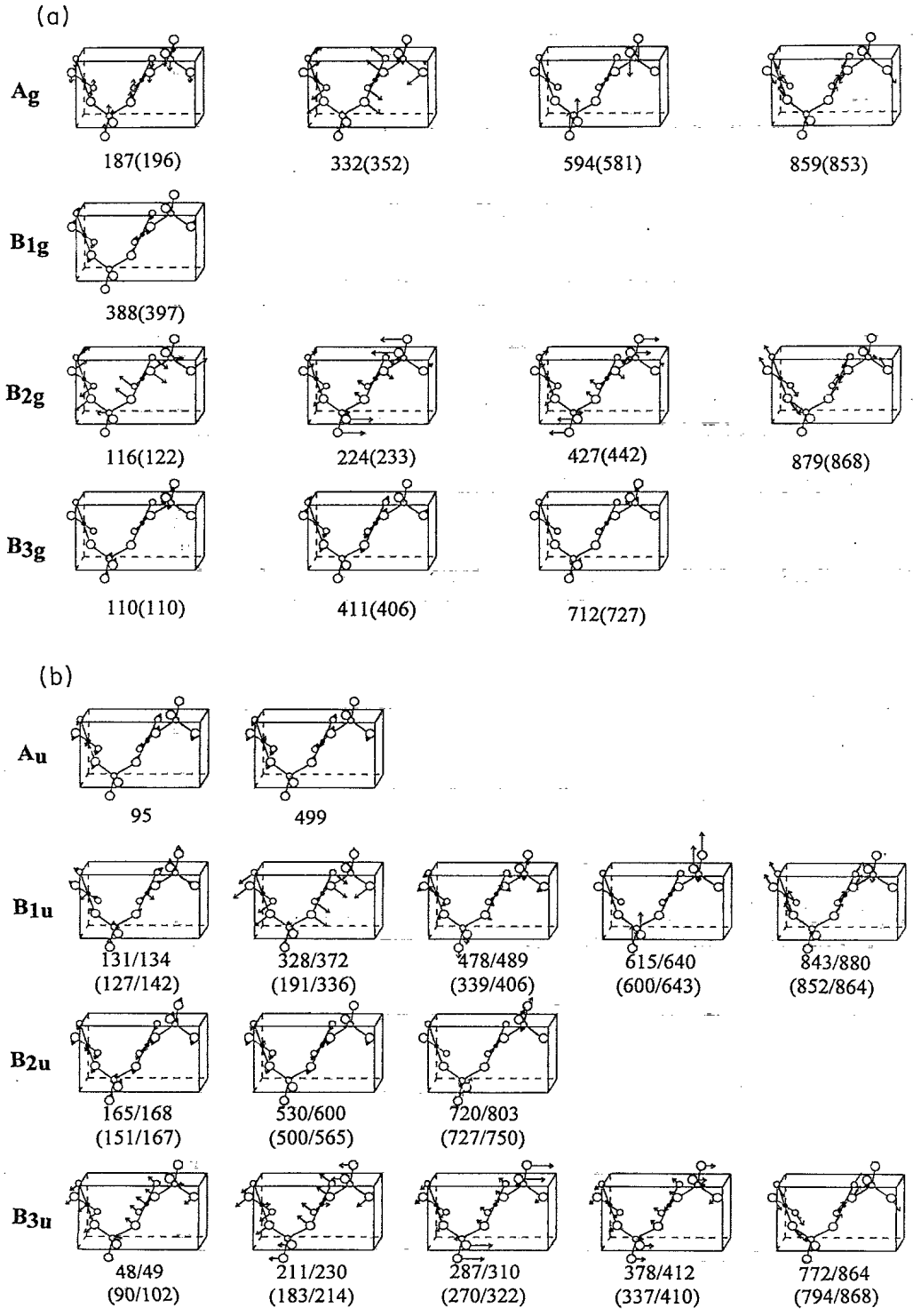

FIG. 4. Normal-mode displacements of $CuGeO_3$ (a) Raman active modes, (b) infrared active modes. Phonon frequencies are in cm^{-1}; the calculated values are given in parentheses.

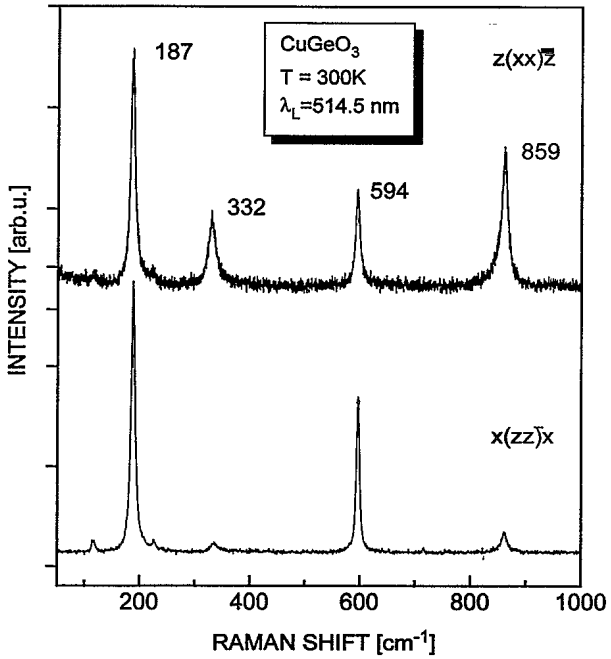

FIG. 5. Room-temperature polarized Raman spectra of $CuGeO_3$ in $z(xx)\bar{z}$ and $x(yz)\bar{x}$ configurations.

TABLE III. Frequencies (in cm^{-1}) for some of the doublets of Raman and infrared active phonons together with the respective values of ν_0, Δ, and $(\nu_0/\Delta)^2$.

ν_+	ν_-	ν_0	Δ	$(\nu_0/\Delta)^2$
A_g	B_{1u}			
332	328	330	36	82.5
594	615	605	113	29
859	843	851	117	53
B_{2g}	B_{3u}			
224	211	218	53	17
427	377	403	142	8
B_{3g}	B_{2u}			
712	720	716	76	89.5

tion the intensity of the A_g^3 mode is at least five times higher then the intensity of the A_g^4 mode.

As we previously noted[10] the B_{1g} symmetry mode originates from out-of-phase oxygen (O_2) atom vibrations [bond bending, see Fig. 4(a)] in CuO_4 squares. The B_{2g} mode eigenvectors are also shown in Fig. 4(a). The first B_{2g} mode comes dominantly from Ge vibration with some contribution of (O_2) atom vibration. The other three B_{2g} modes are scissorlike, bond-bending and antistretching modes of oxygen atom vibration.

The B_{3g} modes are mainly bond-bending vibrational modes which are polarized along the b axis, as is shown in Fig. 4(a). The fact that B_{3g} modes have b axis and B_{2g} modes ac-plane polarization explains why in (xy) configuration,[10] besides the B_{1g} mode, dominantly leak B_{2g} and in (yx) B_{3g} modes, see Fig. 3(b).

The normal coordinates for infrared active phonon modes are given in Fig. 4(b). The low-frequency modes originate from the Cu/Ge atom vibration, the modes with frequencies between 200 and 400 cm^{-1} come from Cu-O vibration and modes at frequencies above 400 cm^{-1} are oxygen vibration. The ionic displacements of all IR active modes are shown in Fig. 4(b).

The great number of different displacement patterns can be reduced to several distinct ones bearing in mind that there are two formula units per unit cell. As a result, each mode of the separate formula unit gives rise to the Davidov pairs. Namely, as previously noted the basic building blocks of $CuGeO_3$ crystal structure are $(GeO_3^{2-})_n$ chains linked by Cu^{2+} ions. There are two of these chains [of $C_{2v}(z)$ symmetry] per unit cell, each with a single GeO_3 repeat unit. According to the compatibility diagram[7,14] between chain $[C_{2v}(z)]$ and crystal symmetry (D_{2h}), and A_1, B_1, and B_2 chain modes split into A_g-B_{1u}, B_{2g}-B_{3u}, and B_{3g}-B_{2u} crystal doublets, respectively. These doublets are given in Table III, where a (4–40) cm^{-1} frequency difference between corresponding Raman (ν_+) and infrared (ν_-) modes can be observed. Table III also contains entries for ν_0, Δ, and $(\nu_0/\Delta)^2$ that are defined in terms of $\nu_\pm$ by the following simple relationship:[14]

$$\nu_\pm=(\nu_0^2\pm\Delta^2)^{1/2},$$

valid for a pair of weakly coupled identical oscillators where ν_0 is the isolated-oscillator frequency and Δ^2 is proportional to the coupling force constant. The ratio of intralayer to interlayer bonding strengths is proportional to $(\nu_0/\Delta)^2$. The mean value of the $(\nu_0/\Delta)^2$ in Table III is approximately 50, indicating that the bonds within a layer are about 50 times stronger than interlayer bonds. This explains a layerlike character of crystal structure of $CuGeO_3$.

After the completion of the work presented here, a Raman-scattering study[15] of the $CuGeO_3$ came to our attention. These results confirm the Raman mode assignment presented in Sec. III.

IV. SUMMARY

The polarized far-infrared reflectivity and Raman-scattering spectra of $CuGeO_3$ are presented. The assignment of the observed modes is given according to the factor-group analysis and normal coordinate analysis based on the shell-model lattice dynamical calculation. The frequency difference of Raman-infrared Davidov doublets yields an intralayer-to-interlayer bond strength of about 50.

ACKNOWLEDGMENTS

We are grateful to W. König and A. Breitschwerdt for measuring FIR and IR spectra and Dr. M. Konstantinović and Dr. M. Abrashev for useful discussions. G.D. and A.R. thank NEDO for the financial help. This work was supported by the Serbian Ministry of Science and Technology under Project No. 0104.

[1]M. Hase, I. Terasaki, and K. Uchinokura, Phys. Rev. Lett. **70**, 3651 (1993).

[2]J. P. Pouget, L. P. Regnault, M. Ain, B. Hennion, J. P. Renard, P. Veillet, G. Dhalenne, and A. Revcolevschi, Phys. Rev. Lett. **72**, 4037 (1994).

[3]K. Hirota, D. E. Cox, J. E. Lorenzo, G. Shirane, J. M. Tranquada, M. Hase, K. Uchinokura, H. Kojima, Y. Shibuya, and I. Tanaka, Phys. Rev. Lett. **73**, 736 (1994).

[4]K. LeDang, G. Dhalenne, J. P. Renard, A. Revcolevschi, and P. Veillet, Solid State Commun. **91**, 927 (1994).

[5]L. F. Mattheiss, Phys. Rev. B **49**, 14 050 (1994).

[6]H. Völlenkle, A. Wittmann, and H. Nowotony, Monatsh. Chem. **98**, 1352 (1967).

[7]D. M. Adams and P. A. Fletcher, Spectrochim. Acta A **44**, 233 (1988).

[8]S. Sugai, J. Phys. Soc. Jpn. **62**, 3829 (1993).

[9]H. Kuroe, T. Sekine, M. Hase, Y. Sasogo, K. Uchinokura, H. Kojima, I. Tanaka, and Y. Shibuya, Phys. Rev. B **50**, 16 468 (1994).

[10]S. D. Dević, M. J. Konstantinović, Z. V. Popović, G. Dhalenne, and A. Revcolevschi, J. Phys. Condens. Matter **6**, L745 (1994).

[11]A. Revcolevschi and G. Dhalene, Adv. Mater. **5**, 657 (1993).

[12]D. L. Rousseau, R. P. Bauman, and S. P. S. Porto, J. Raman Spectrosc. **10**, 253 (1981).

[13]V. N. Popov, J. Phys. Condens. Matter **7**, 1625 (1995).

[14]Z. V. Popović, Phys. Rev. B **32**, 2882 (1985).

[15]M. Udagawa, H. Aoki, N. Ogita, O. Fujita, A. Shima, A. Ogihara, and J. Akamitsu, J. Phys. Soc. Jpn. **63**, 4060 (1994).